Science of the Total Environment 485–486 (2014) 828–841

Contents lists available at ScienceDirect

Science of the Total Environment

journal homepage: www.elsevier.com/locate/scitotenv

Challenges to estimate surface- and groundwater flow in arid regions: The Dead Sea catchment

Christian Siebert [a,*], Tino Rödiger [a], Ulf Mallast [a], Agnes Gräbe [a], Joseph Guttman [b], Jonathan B. Laronne [c], Yael Storz-Peretz [c], Anat Greenman [d], Elias Salameh [e], Marwan Al-Raggad [e], Dina Vachtman [f], Arie Ben Zvi [g], Danny Ionescu [h], Asher Brenner [c], Ralf Merz [a], Stefan Geyer [a]

[a] Helmholtz Centre for Environmental Research–UFZ, T. Lieser Str. 4, Halle 06120, Germany
[b] Mekorot Co. Ltd, 9 Lincoln St, Tel Aviv 61201, Israel
[c] Department of Geography and Environmental Development, Ben Gurion University of the Negev, Beer-Sheva 84110, Israel
[d] Lower Jordan River Drainage Authority, Beit Hashita, Israel
[e] University of Jordan, Al Jamia Al Urduniyya Amman, Kingdom of Jordan
[f] Department of Earth Sciences, University of Bergen, Bergen, Norway
[g] Sammy Shamoon College of Engineering, Beer Sheva, Israel
[h] Max-Planck Institute for Marine Microbiology, Bremen, Germany

HIGHLIGHTS

- This paper presents a trans-boundary approach to evaluate water fluxes into the Dead Sea.
- Independent methodologies were chosen to close the gap of data scarcity.
- The combination of remote sensing and fingerprinting reveals new insights into the submarine groundwater appearances.
- Regionalised recharge simulations permit preparation of future scenarios based on forecasted reduced precipitation.

ARTICLE INFO

Article history:
Received 27 February 2014
Received in revised form 1 April 2014
Accepted 2 April 2014
Available online 22 April 2014

Editor: D. Barcelo

Keywords:
Dead Sea
Groundwater flux
Surface runoff
Submarine springs
Recharge simulations

ABSTRACT

The overall aim of the this study, which was conducted within the framework of the multilateral IWRM project SUMAR, was to expand the scientific basement to quantify surface- and groundwater fluxes towards the hypersaline Dead Sea. The flux significance for the arid vicinity around the Dead Sea is decisive not only for a sustainable management in terms of water availability for future generations but also for the resilience of the unique ecosystems along its coast.

Coping with different challenges interdisciplinary methods like (i) hydrogeochemical fingerprinting, (ii) satellite and airborne-based thermal remote sensing, (iii) direct measurement with gauging station in ephemeral wadis and a first multilateral gauging station at the river Jordan, (iv) hydro-bio-geochemical approach at submarine and shore springs along the Dead Sea and (v) hydro(geo)logical modelling contributed to the overall aim.

As primary results, we deduce that the following:

(i) Within the drainage basins of the Dead Sea, the total mean annual precipitation amounts to 300 mm a^{-1} west and to 179 mm a^{-1} east of the lake, respectively.
(ii) The total mean annual runoff volumes from side wadis (except the Jordan River) entering the Dead Sea is approximately 58–66 × 10^6 m^3 a^{-1} (western wadis: 7–15 × 10^6 m^3 a^{-1}; eastern wadis: 51 × 10^6 m^3 a^{-1}).
(iii) The modelled groundwater discharge from the upper Cretaceous aquifers in both flanks of the Dead Sea towards the lake amounts to 177 × 10^6 m^3 a^{-1}.
(iv) An unexpected abundance of life in submarine springs exists, which in turn explains microbial moderated geo-bio-chemical processes in the Dead Sea sediments, affecting the highly variable chemical composition of on- and offshore spring waters.

The results of this work show a promising enhancement of describing and modelling the Dead Sea basin as a whole.
© 2014 Elsevier B.V. All rights reserved.

* Corresponding author. Tel.: +49 345 5585211.
E-mail address: christian.siebert@ufz.de (C. Siebert).

http://dx.doi.org/10.1016/j.scitotenv.2014.04.010
0048-9697/© 2014 Elsevier B.V. All rights reserved.

1. Introduction

The riparians of the Dead Sea suffer from semiarid to arid climatic conditions with serious shortages of high-quality freshwater resources, aggravated by a dense and increasing population. However, to ensure the socioeconomic stability, intense exploitation of available water resources is necessary. That, in turn, requires a detailed knowledge about the amounts and mechanisms of fresh groundwater flux and the amount of surface runoff that results from precipitation. Consequently, a humongous amount of surveys were performed on that topic in the Dead Sea basin (among others, Al-Weshah, 2000; Avrahamov et al., 2010; Burg, 2006; Enzel et al., 2006; Frumkin et al, 2011; Gavrieli et al., 2001; Gvirtzman and Stanislyvsky, 2000; Katz and Starinsky, 2008; Laronne Ben-Itzhak and Gvirtzman, 2005; Lensky et al., 2005; Möller et al., 2003, 2007; Niemi et al., 2009; Oz et al., 2011; Salameh and El-Nasser, 1999, 2000; Salameh and Al Farajat, 2006; Shaliv et al., 2006; Yechieli, 2000; Yechieli et al., 1995, 2006, 1996). The *Best Available Data Report*, mutually published by the Tahal Group and the Geological Survey of Israel (TAHAL, 2010), conveys a comprehensive overview. Our below described approach relates to adding knowledge, on aspects that were or could not be gained before.

The hypersaline Dead Sea (total dissolved solids [TDS] = 367 g l^{-1}) is a terminal lake, situated within the Jordan–Dead Sea Rift (DSR) system. The lake consists of a deep northern basin (deepest point at −725 m mean sea level (msl.)) and a shallow southern basin. The latter would have been dried out but is artificially sustained by continuous pumping of water from the northern basin as it is used for commercial mineral production. Since the onset of dramatic anthropogenic interventions into the regional hydrological equilibrium during the 1960s, the natural northern basin, with a current (2013) water level at −427 m msl, continuously shrinks. As result of failure of the international community and the riparian countries, mainly the Jordan River, which was and is the major contributor to the lake, was subject to a row of unilateral water management schemes that reduced the discharge of the remaining Jordan River by about 90% from naturally >1,370 × 10^6 m^3 a^{-1} (Salameh, 1996) to 16–400 × 10^6 m^3 a^{-1} (Asmar and Ergenzinger, 2002; Holtzmann et al., 2005):

- In 1955–1964, King Abdullah and East Ghor Canals were constructed in the Kingdome of Jordan to divert about 25% of the natural flow of Yarmouk River (main contributor to the Lower Jordan River).
- In 1964, Lake Tiberias was embanked, which reduced its effluent and the resulting Lower Jordan River (LJR) by 90%, compared to the amount of water that left the lake prior to the dam.
- In 2009, Syria and Jordan reduced the discharge of the Yarmouk River again by the finalization of the Al-Wahda dam (Al-Taani, 2013) and several small-scale retention structures in the tributaries of the Yarmouk River.

Additionally, water budget influence originates from dam constructions in wadis along the eastern side of the Dead Sea (DS) and the growing potash companies in Jordan and Israel pumping out 500 × 10^6 m^3 a^{-1} from the Dead Sea into evaporation pans and restore about 250 × 10^6 m^3 a^{-1} of concentrated brines back (Lensky et al., 2005).

The resulting effects on the natural equilibrium of the Dead Sea were dramatic. While lake level under natural conditions (until 1950s) fluctuated negligibly around −395 m msl. (EXACT, 1998), the human impact dramatically reduced the amount of inflowing water. Accelerated by the high evaporation of 1.1–1.2 m a^{-1} (Lensky et al., 2005), the lake declines by ca. 1 m a^{-1}, comparable to 700 × 10^6 m^3 a^{-1} of volume loss (Gavrieli et al., 2006). As a serious effect, connected groundwater tables in surrounding mountain aquifers dropped accordingly (Yechieli et al., 2010). These fresh groundwaters discharge from the mountain aquifers and pass the recently exposed lakebed inducing suberosion structures that endanger infrastructure and tourism (Yechieli et al., 2006). Moreover, the dropping groundwater levels cause a vegetation dieback and desiccation of springs threatening endemic life in still existing ecosystems such as Ein Feshkha/Enot Zuqim along the shoreline.

Measurements of groundwater discharge along the shoreline of the lake cover the known onshore springs only (HSI, 2012). Submarine groundwater discharge, although visible, was not quantitatively detected yet. Similarly, gauging surface runoff is challenging, as there is only episodic water flow. If temporal runoff occurs, the measurement is pursued in an extreme environment with torrential water flow, accompanied by intense sediment transport. As a consequence, the time series of measurements of ephemeral wadi flows are almost not available.

Consequently, despite long, intense and valuable efforts carried out to investigate the effects of the dropping Dead Sea level on surrounding essential water resources, the complexity of interacting systems and the difficulty to measure certain states variables hindered to comprehensively determine amounts of surface runoff and groundwater discharge. These still open questions led to the here presented project, performed by a multilateral research team from Jordan, Israel, Palestine and Germany. Large efforts were undertaken to realise a holistic approach by combining evaluations of input (precipitation), transfer (recharge and surface runoff) and output (groundwater discharge) of water fluxes through ephemeral wadis, the surrounding aquifers and the exposed lakebed. An extensive geological database was developed and consequently high-resolution structural models for the upper Cretaceous aquifers on both sides of the lake were derived. On this basis, we built regional numerical groundwater flow models to investigate the groundwater regime in the Dead Sea drainage basin.

1.1. Hydrogeology of the study site

The western flank of the Dead Sea is represented by a mountain range, building the N-S-oriented backbone of Israel's and Palestine's water supply. It hosts two major lime- and dolostone aquifers of upper Cretaceous age, which crop out along the flank and beneath a buried lower Cretaceous sandstone aquifer. Inside the Graben, Quaternary fluviatile sediments around wadi mouths interfinger with the lacustrine to hypersaline lake sediments that form the heterogeneous coastal Dead Sea Group (DSG) aquifer (Fig. 1). Within the flank, structural features, observable as surface lineaments, may represent preferential groundwaters flow paths from recharge areas in the west towards the Dead Sea (Mallast et al., 2011) (Fig. 1A). At these locations, groundwater preferentially discharges from the DSG in large spring areas: Ein Feshkha, Kane/Samar, Mizpe Shalem, Qedem and Ein Gedi. In general, two spring types occur: (i) terrestrial springs, emerging along faults or sediment heterogeneities that incise erosion channels within the dry-fallen DSG sediments, and (ii) submarine springs that emerge on the lake's bottom in depths at least down to 30 m below lake level (Ionescu et al., 2012), establishing a density-driven buoyancy flow that can form visible circular patterns on the DS surface (Munwes et al., 2010) (Fig. 1B).

Groundwaters along the eastern flank occur within the equivalents of the west: (i) the lower Cretaceous sandstone and (ii) the upper Cretaceous limestone aquifer, respectively. However, contrastingly to the west, the lower Cretaceous sandstones crop out along the eastern shoreline. That sandstone aquifer, together with beneath situated older mostly sandy formations, forms the “lower aquifer,” which discharges through springs along the Dead Sea and within wadis (e.g., Zarqa Ma'in, Mujib, Wala, Shaqiq and Ibn Hammad). Its current replenishment is very low since its recharge occurs through the outcrops in the arid S and SE of Jordan (Salameh and Hammouri, 2008). Contrastingly, the upper Cretaceous limestone aquifer is replenished by recent precipitation in the eastern Graben shoulder and discharges after residence times of only some years (Ereifeg, 2006). While its natural discharge only occurs through some springs mainly in the headwaters of the wadis, its anthropogenic exploitation by pumping wells is essential for the socioeconomic welfare of Jordan.

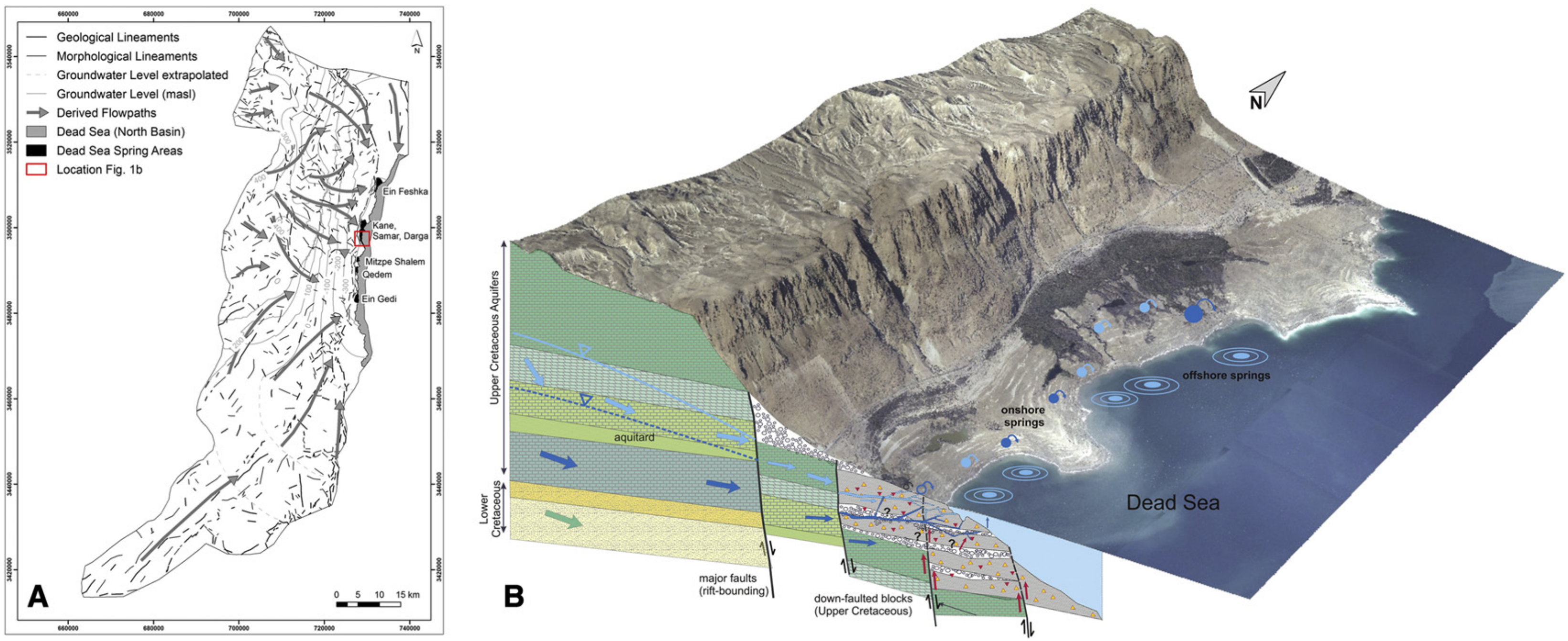

Fig. 1. Shows (A) derived groundwater flow-paths and the corresponding spring areas along the northern basin of the Dead Sea. In red, the approximate location of Fig. 1B is indicated and (B) a 3D graph of the Kane/Samar/Darga area, with on- and offshore springs and a conceptual geological cross section to imagine location of aquifers. Satellite image: RapidEye, DEM: this study.

All together, the natural discharge values along the eastern flank $30–90 \times 10^6\ m^3\ a^{-1}$ (Salameh, 1996; Lensky et al., 2005) are proposed to be similar to those along the western flank $80–120 \times 10^6\ m^3\ a^{-1}$ (Lensky et al., 2005; HSI, 2012).

1.2. Hydrology of the study site

Surface water inputs to the DS are limited to the perennial Jordan River entering from the north and ephemeral flash floods in Wadis (Fig. 2; Table 1) generated after significant precipitation events during the rainy season (October–April) (Gertman and Hecht, 2002). The Dead Sea area is characterized by an infrequent, high-intensity flood regime with extreme hydrographs. Due to the southwards increasing aridity, the situation is sharpened for the southern Wadis, which may be dry even for several years (Cohen and Laronne, 2005). Wadis draining towards the Dead Sea carry very high concentrations of suspended sediment, typically 50–200 g l^{-1}. The yield of bedload (coarse sand to boulders) in these wadis is exceptionally high even at low discharges (Cohen and Laronne, 2005), which is the result of lacking armoring and the morphotexture of finer sediment in the channels and coarser sediment on the bars (Storz-Peretz and Laronne, 2013).

The surface runoff volumes of the direct DS-drainage basin (excluding Jordan River) vary from 5 to $256 \times 10^6\ m^3\ a^{-1}$ (Lensky et al., 2005; Greenbaum et al., 2006), with respective rates of $1–30 \times 10^6\ m^3$ per flood event (Greenbaum et al., 2006).

Table 1
Catchment characteristics along the Dead Sea.

Number in Fig. 1	Name (hebrew)	Name (arabic)	Size (km^2)
1	Og/Qumran	Og/Qumeran	160
2	Qidron/Samra		120
3	Darga		230
4	Hazezon/Qedem		97
5	Arugot/David	Al-Ghar	248
6	Hever/Mishmar	Abu El-Hayyad	216
7	Ze'elim		280
8	Rahaf/Mezada		92
9		Hisban	ca. 250
10		Zarqa Ma'in	272
11		Wala	2,000
12		Mujib	4,600
13		Shuqeiq	ca. 180
14		Ibn Hammad	125
15		Karak	190
16		Hasa	2,520
17	Heimar		360

2. Methods

Quantifying water fluxes towards the Dead Sea is difficult, which required the development of new methodological solutions. These solutions comprising information from gauging stations, remote sensing data, hydrochemical fingerprinting and modelling exercise are briefly

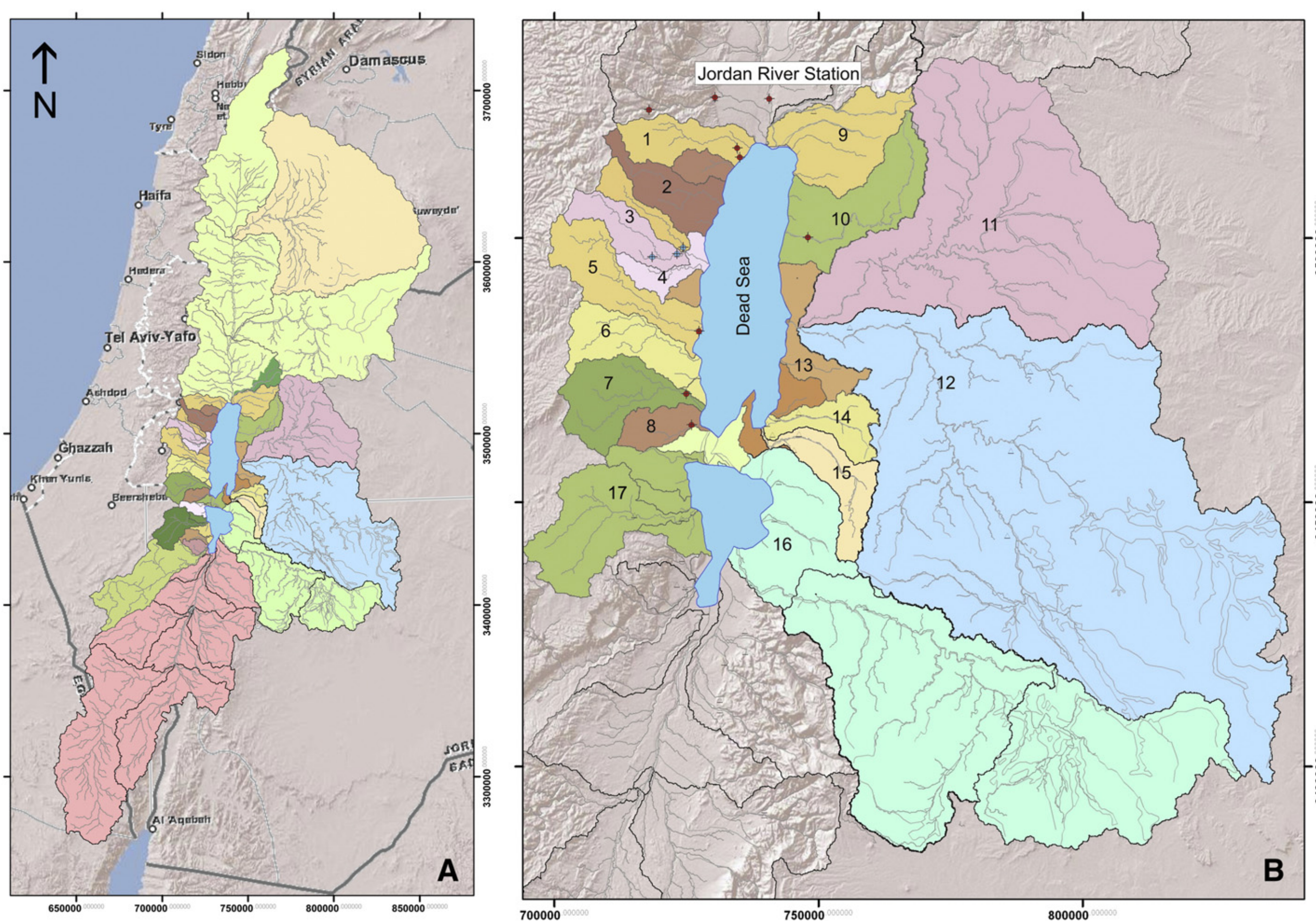

Fig. 2. Shows (A) the complete drainage basin of the Dead Sea including Jordan River and Yamouk drainage basins in the north and (B) the direct drainage basin with side Wadis. Numbers are explained in Table 1, dots indicate runoff gauging stations of this study (red) and of authorities (blue).

described below and can be found elaborately described in the given publications, respectively.

(A) Manual or automatic recording of ephemeral surface runoff that occurs spatially scattered and only sporadically is not possible since events are very short and carry high sediment loads with a strong potential of damage. Hence, only stage can be automatically monitored and must be translated into discharge. Therefore, 8 gauging stations have been installed in side wadis (red dots in Fig. 2), to measure stage, electrical conductivity, temperature and suspension load of flash floods. We selected those wadis to be equipped, which represent prior investigated changes in aridity, morphology and geology well (Storz-Peretz et al., 2011; Storz-Peretz and Laronne, 2013). Following the selection, an R-based statistical multi-regression approach was applied evaluating the sensitivity of wadi characterising physical parameters on runoff (Greenman, 2010).

(B) The only perennial Lower Jordan River is inaccessible on a regular base as it represents the country frontier in most parts of its course. Due to political and security reasons within that context, discharge measurements requiring determination of riverbed morphology (cross-sections) and velocity profiles were not possible. However, we were able to install the first hydrometric station in the Jordan River, which is comparable to those in ephemeral streams.
For both, ephemeral runoff and Jordan River, the inoperativeness of inductive or mechanical devices to pursue manual measurements of stream velocity led to the successful application of radar velocimetry (Zamler and Laronne, 2010).

(C) To evaluate the discharge from groundwater springs along the lakeshore, a mobile Marsh McBirney Flo-Mate was used at accessible springs in combination with streambed dimensioning. Stationary ultrasonic Doppler instruments (Unidata 6562B) were applied to continuously monitor water depth, depth-averaged flow velocity and water temperature in three springs during 2004–2006 (Vachtman and Laronne, 2013a). However, many springs are (i) inaccessible due their deep incision into the soft sediments, (ii) too diffuse to pursue proper measurements or (iii) yet unknown (concerns mainly submarine springs). Hence, we developed approaches to evaluate discharge through mono-temporal air (uncooled microbolometer—Infratec VarioCam hr) and multi-temporal satellite-based (Landsat ETM + band 6.2) thermal remote sensing. For both approaches, the underlying principle exploits (i) the thermal contrast between discharging groundwater and the DS and (ii) the sea-surface temperature stabilization within a certain area off the discharge outlet due to the constant groundwater temperature (Mallast et al., 2013a, 2013b).

(D) To chemically differentiate between types and the origin of discharging groundwaters, on- and offshore springs were sampled. We combined hydrochemical methods, including rare earth element + yttrium (REY) fingerprinting, isotopic and microbial studies. However, rare earth elements including yttrium (REY) were sampled onshore and with the help of divers also offshore by using peristaltic pumps. Samples were filtered (Sartorius Sartobran 0.2 μm) and acidified to pH 2 (Merck HCl suprapure) on site, subsequently enriched by using ion-exchange columns and finally analysed using ICP-MS. The analytical procedure is elaborately described in Siebert et al. (2012). Simultaneously, samples for microbial community screening have been taken as explicitly described in Ionescu et al. (2012).

(E) The numerical evaluation of the surface and groundwater flow-dynamics and fluxes, respectively, were pursued using a regional hydrological model for the western surface basin (JAMS (Kralisch and Krause, 2006) and a TRAIN-ZIN (Lange, 1999; Menzel, 1997) simulation for the eastern surface drainage basin. Groundwater flow was simulated for the upper Cretaceous aquifers in the eastern and western subsurface Dead Sea basins, respectively (Al-Raggad, 2009; Odeh et al., 2009, 2010; Sachse et al., 2013) by adopting WASI Feflow 6.1.

3. Results and discussion

3.1. Precipitation

To calculate recharge and rainfall–runoff correlations, climate characteristics and rainfall distribution, which are highly variable, data sets from all available 41 precipitation stations in the region (own station network, Israel Met. Surv., Palestine Met. Surv., Jordan Met. Surv., www.wunderground.com, www.tutiempo.net, metbroker, NOAA) have been regionalised. The average rainfall decreases from north to south and, in the western flank due to the rain shadow effect, with decreasing elevation from about 650 mm a^{-1} in the west to less than 50 mm a^{-1} (14 mm a^{-1} in Ein Gedi at the DS) close to the lake (Fig. 3). The amount of rainfall and resulting groundwater recharge was calculated on the lateral extents of the subsurface catchments of the upper Cretaceous aquifers: in the west, 3,820 km^2; in the east, 3,427 km^2. The resulting total mean annual precipitation volumes for the period 1979–2010 were $1{,}166 \times 10^6$ m^3 a^{-1} (300 mm a^{-1}) in the west and 616×10^6 m^3 a^{-1} (179 mm a^{-1}) in the east. Although areas on both sides are relatively similar in their extension, the amount of precipitation is different, probably due to the extremely fast declining precipitation amounts towards the Jordan Dessert in the East (Fig. 3).

3.2. Surface runoff into the Dead Sea

Although several wadis draining towards the Dead Sea were or are equipped with runoff gauging stations, only poor data series are available. Along the western side, long-term series for undisturbed (no sewage drainage) wadis were only available for the Wadis Rahaf (1991–2012), Arugot (1990–2001, 2009–2012) and Darga (1991–2012) (3 out of 9 wadis, ref. Table 1); on the Jordanian side, none was available. To overcome data scarcity, within this study, Wadis Og, Ze'elim and Arugot (all W of DS) and Zarqa Ma'in (E of DS) were equipped with gauging stations at their outlets from the mountain range. The received short-term series provided sufficient data sets to calibrate local hydrological models, simulating the respective catchment runoff.

However, local synoptic systems causing intense spatial and temporal precipitation heterogeneity and likewise resulting runoff differences between wadis contradict a simple extrapolation of the measurements to from gauged to ungauged wadis. Consequently, we applied a generalized Pareto distribution on a partial duration series (short-term series for winters 2007/2008 and 2008/2009) to assess the annual runoff volume under co-consideration of the probability weighted moment method to estimate included parameters. The considered parameters that were selected based on data availability are as follows: size of watershed, elevation, latitude and meridian at the top of the main channel, topography, mean annual precipitation and mean annual number of runoff events per watershed. The contribution extent of each parameter to the correlation was determined by multiple regression (Greenman, 2010).

It reveals that the most significant parameters controlling the expected discharge volumes in the respective catchments are drainage area and meridian. Due to the meridional extension of the mountain ranges straddling the DS, the longitudinal location (E-coordinate of Israel Transverse Mercator coordinate system; expressed in integer km) of the top of the main channel reflects the elevation of the drainage divide. Applying the derived multiple regression Eq. (1) on the western direct surface drainage basin (1,443 km^2; Table 2; basins 1–8 in Fig. 2B),

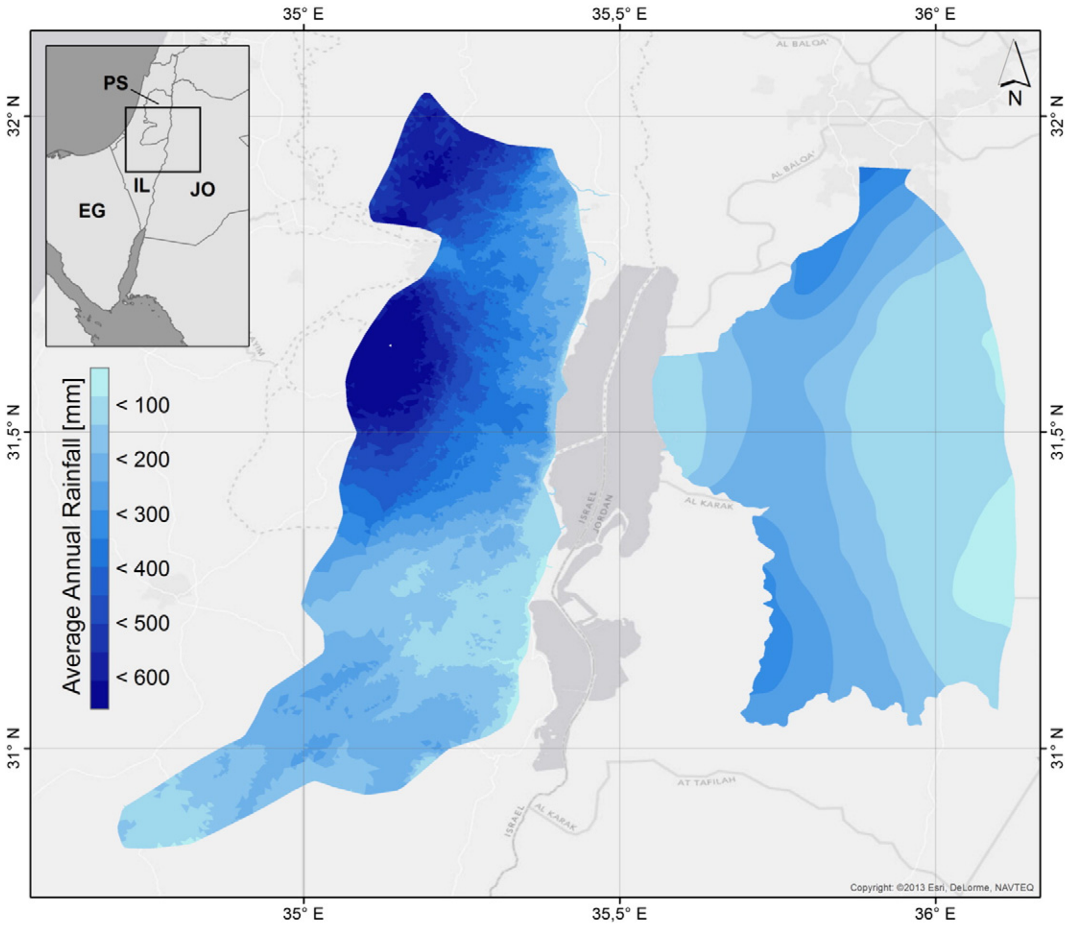

Fig. 3. Rainfall distribution on both sides of the Jordan Graben for the period 1979–2010.

the long-term mean annual discharge from all the western wadis was calculated to be 2.7×10^6 m^3 a^{-1}, being equal to 1.9 mm a^{-1}.

$$V(a) = 2.01637A–0.00349M \quad (1)$$

where $V(a)$ = expected annual surface runoff volume per station (10^3 m^3 a^{-1}), A = drainage area (km^2) and M = meridian (longitudinal coordinate in integer km).

To evaluate the above described basic empirical approach on short-term data for 2 rainy seasons, the process-based hydrological model JAMS was applied on long-term data sets (1978–2010). The model takes morphology, land cover, soil parameters and climatic data into account and was calibrated against the measured hydrographs of gauged catchments. The resulting annual discharge for the period 1978–2010 amounts to 15.4×10^6 m^3 a^{-1} for the direct western surface drainage basin (1,443 km^2), corresponding to 10.7 mm a^{-1}.

The considerable differences between both approaches may reflect the importance of long-term data sets of precipitation. The rainy seasons in calculation periods 2007–2009 were relatively dry, compared to the average of 300 mm a^{-1} (Fig. 4). Hence, the received runoff (1.9 mm a^{-1}) from statistical evaluation by far underestimates the modelled surface runoff from the direct western drainage basin. Taking the runoff/precipitation ratio (Table 2) as reference, the empirical approach yields a ratio value of 0.006, while the process-based approach exhibits a value of 0.036 that is supported by the ratio value of 0.02 derived by an independent study of Morin et al. (2009).

The existing station network in Jordan unfortunately offers no gauging stations at wadi outlets. This fact and large difficulties to install new hydrometric stations along the eastern flank impeded the application of the methods described above.

However, by combining locally varying (0.01–0.07) runoff/precipitation ratios from GTZ and NRA (1977) with recent precipitation data, an average of 25×10^6 m^3 a^{-1} for the 3,427 km^2 large subsurface basin of the upper Cretaceous aquifer in the eastern flank was calculated. It was necessary to discretise the area concerning their respective runoff/precipitation ratios as their variation depends on morphology and land cover, leading to the higher values in headwaters compared

Table 2
Surface runoff calculations for given drainage areas in both flanks.

Calculation area	Reference	Area (km^2)	Runoff (10^6 m^3 a^{-1})	Ratio (mm a^{-1})	Runoff/precipitation ratio
Western SDB*	Greenman (2010)	1,443	2.7	1.9	0.006
Western SDB*	Sachse et al. (2013)	1,443	15.4	10.7	0.036
Eastern SDB	Alkhoury (2012)	6,277	51	8.1	0.045
Eastern SDB#	Al-Raggad (2009)	3,427	25	7.3	0.041

* SDB: surface drainage basin of the northern DS basin,
\# Subsurface basin of the upper Cretaceous aquifer only.

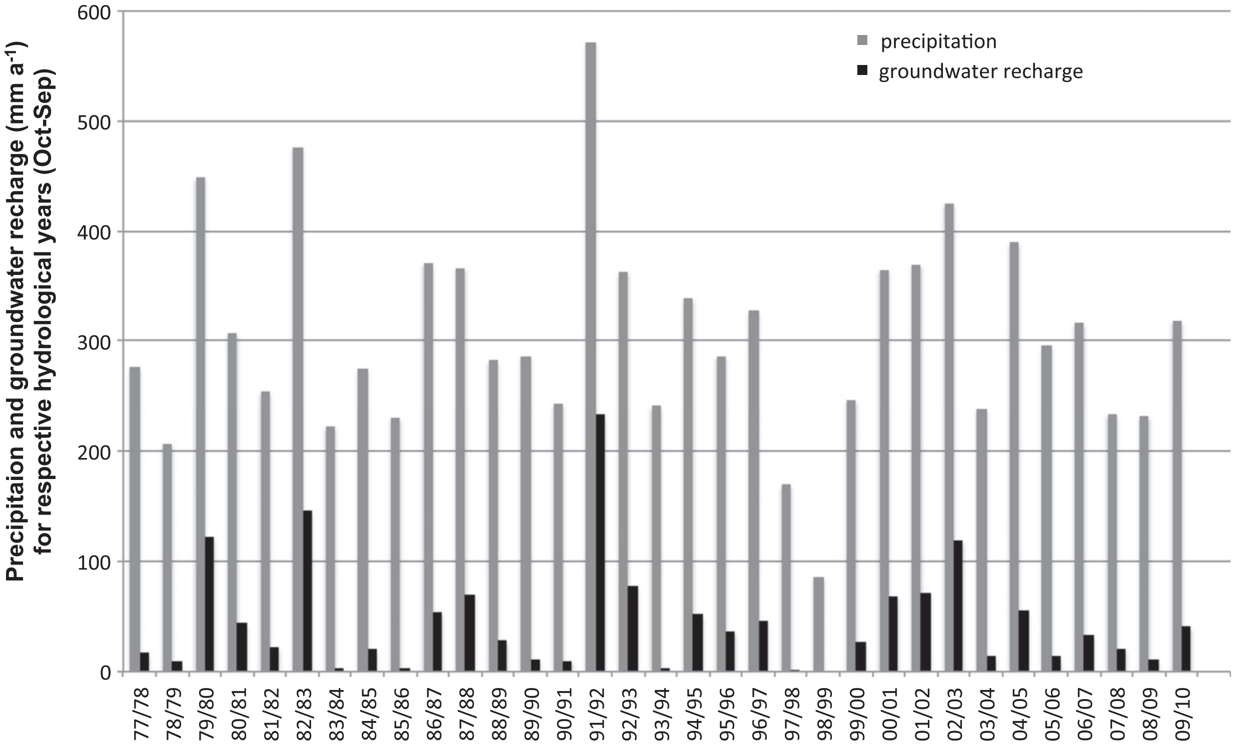

Fig. 4. Time series of precipitation and JAMS-simulated recharge for the hydrological years (October–September) 1977/1978–2009/2010.

to wadi sections closer to the Dead Sea (Al-Raggad, 2009). The average ratio was 0.04, resulting in runoff of 7.3 mm a^{-1}.

Due to the fact that the entire direct eastern surface drainage basin (6,227 km^2) nearly doubles the subsurface basin of the upper Cretaceous aquifer, a non-calibrated TRAIN-ZIN model was additionally set up for the large area. By taking data sets for the period 1966–2006, Alkhoury (2012) estimated a mean annual surface runoff from the eastern mountains towards the Dead Sea to be 51×10^6 m^3 a^{-1} corresponding to 8.1 mm a^{-1} with a runoff/precipitation ratio of 0.045 (Table 2).

Not included in these calculations were (i) Wadi Arava, as an enormous amount of water is lost due to transmission loss (Greenman, 2010), and (ii) the Jordan River as its annual discharge numbers differ widely between 16 and 400×10^6 m^3 a^{-1} (Asmar and Ergenzinger, 2002; Holtzmann et al., 2005). Because of the tremendous importance of that only perennial river of the DS basin, we intended and eventually build up a hydrometric station 8 km upstream the mouth of the Jordan River, at the Baptism Site. Since the Lower Jordan River is representing an international border in the Middle East, it is quasi flowing through no man's land. Consequently, nearly insuperable political and military obstacles had to be smoothed. Finally, in 2010, we were successful to install the equipment (level meter, electrical conductivity, temperature, turbidity sensors and an automatic water sampler) within the stream (Figs. 2B and 5). To permit the station to be virtually accessible for all project partners, automatically logged values are transferred to a login-protected Web site, which will be shifted to public domain access soon. However, due to military restrictions, we were not allowed yet to pursue continuously depth and velocity measurements to obtain absolute discharge values and to derive a reliable stage-discharge correlation function. During the years 2010 and 2011, we had one chance to take a velocity profile, resulting in preliminary amounts of 60 and 172×10^6 m^3 a^{-1} for each year, respectively. If once the permission will be granted, the station will be upgraded to automatically support the scientific community with reliable discharge volumes in real time and subsequently will provide answers to one of the most important questions in the Dead Sea water balance.

3.3. Groundwater—the remote sensing approach

As described above, groundwater discharges through onshore and offshore springs along the DS shore, which is in wide parts impassable due to life-threatening genesis of sinkholes or security reasons. To overcome the knowledge gaps concerning groundwater contribution to the lake's budget, we developed a methodology to estimate water discharge from onshore springs. The approach develops a relationship between remotely derived water surface width of the incised channels into the lacustrine DSG sediment bed as a single hydraulic geometry variable and in-situ obtained discharge measurements (Vachtman and Laronne, 2011, 2013a, 2013b). Channels in the northern part of the Ein Feshkha area (Fig. 1A), which drain ca. 60% of the entire water discharge of the Nature Reserve, were selected for time-varying discharge examination using ultrasonic Doppler gauging stations. All the in situ measurements of channel geometry and water discharge were performed simultaneously with large-scale aerial photography. Based on calibration of over 400 in situ-derived depth and velocity measurements and simultaneous hydrometric data derived from aerial images, width-discharge rating curves were established, tested and applied to postdict water discharge. The reconstructed trend reveals a major (63%) reduction in average fresh water inflow between 1990 and 2006 (Fig. 6).

Second, we developed a thermal remote sensing approach to identify exact discharge locations. The principle is based on sea surface temperature (SST) contrasts, evoked through steady and season independent, temperature-stable groundwater discharge and varying SSTs of the Dead Sea over time (Mallast et al., 2013a). Regularly measured groundwater temperatures along the western shore (Fig. 1A) in Ein Feshka, Kane and Samar showed 25 °C–28 °C throughout the year (Mazor et al., 1980; this study). Only in the area between Qedem and Mizpe Shalem (Stanislavsky and Gvirtzman, 1999), hot brines with up to 45 °C occur. In contrast, the skin temperature of the DS varies during the year between 23 °C and 30 °C, with a maximum of >34 °C in Aug/Sep (Gertman and Hecht, 2002) (Fig. 7). During high seasons, the thermal gradient between groundwater and lake water is maximised

Fig. 5. Installation of the hydrometric station inside the Lower Jordan River at Baptism Site. Sensor installation and view over the river towards Jordan (upper row), hidden sensor logger and auto sampler (lower row).

and promising for thermal analysis of groundwater inflow. In winter, this fact is particularly enhanced. During that period, fresh to brackish groundwater (density of 1.06–1.19 g cm^{-3}) entering the lake from both terrestrial and submarine ascends to the DS surface as the density differences (DS: 1.24 g cm^{-3}) result in positive buoyancy.

Seen over time as temperature stable groundwater discharges, it stabilizes the SST of a certain area off the discharge location, which results in a small temporal SST variability (Fig. 7). In contrast, areas without discharge locations exhibit a highly SST variability as it follows the seasonal air temperature. Exploiting this difference reveals 37

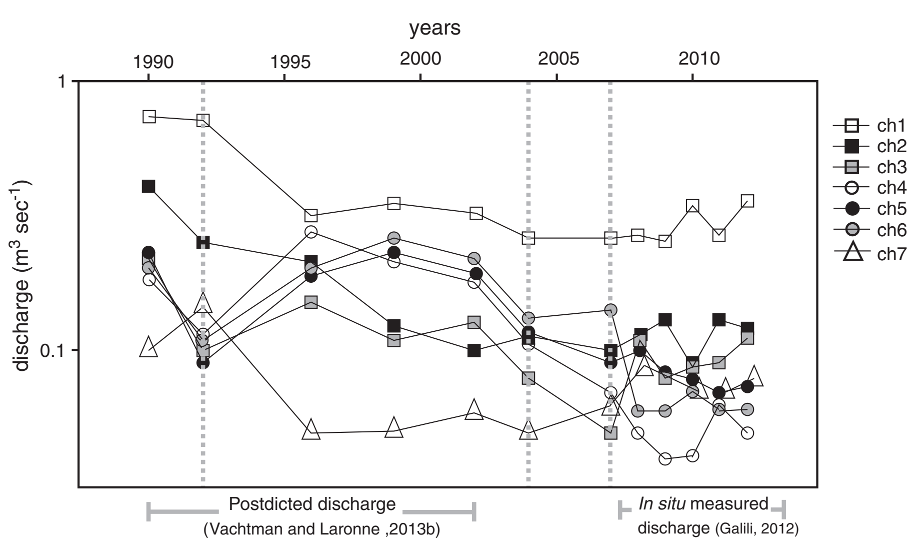

Fig. 6. Calculated changes in stream discharge based on rating curve (Vachtman and Laronne, 2013b). Dotted lines represent years (1992, 2004 and 2006) for which discharge was also measured *in situ*. Discharge data 2006–2011 derived from measurements of the Hydrological Survey of Israel (HSI).

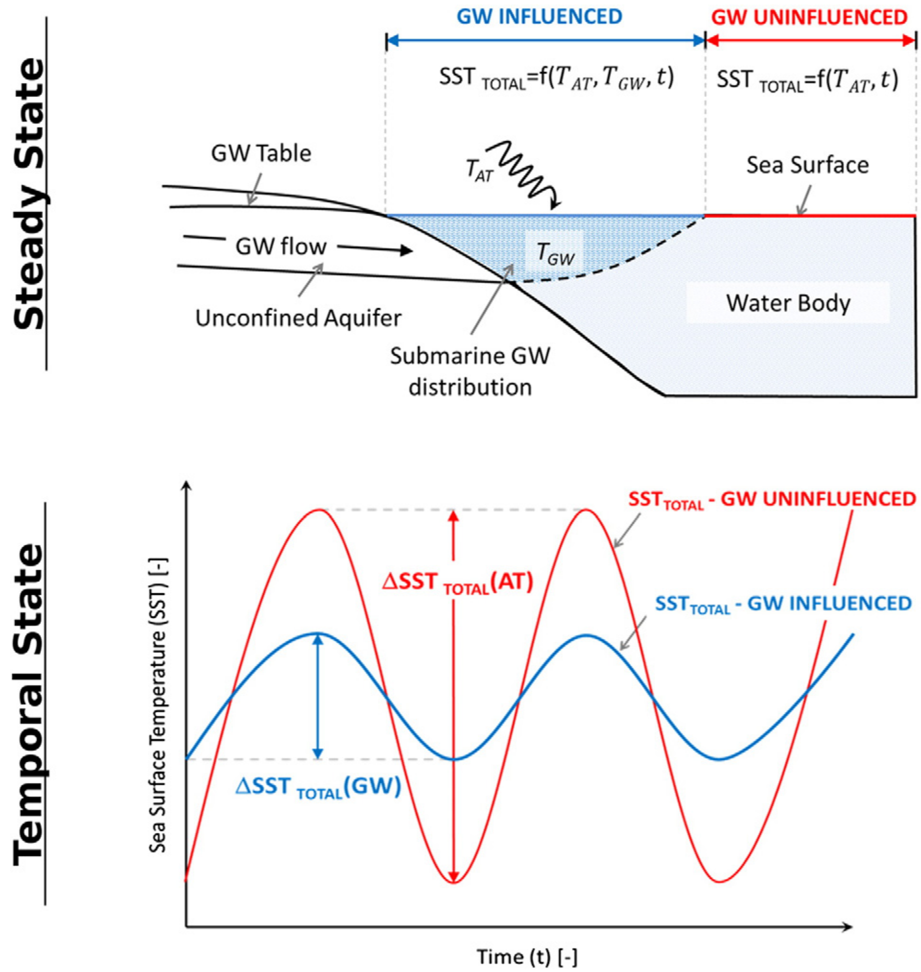

Fig. 7. Schematic generalization of the influence of discharging groundwater on the sea-surface temperature (SST) at steady (upper) and temporal (lower) states. It shows that a continuous and temperature-steady groundwater influx stabilizes the SST off the discharge location and depletes seasonal SST amplitudes leading to minor variability's and small ΔSST values over time compared to groundwater uninfluenced areas.

groundwater discharge sites along the Dead Sea coastline with varying extents that represent variable volumes. The largest two appear along the western coast and correspond to the largest known spring areas of Ein Feshkha and Samar (Fig. 8A and southern part of Fig. 8B) with measured discharge volumes of 82–94 × 10^6 m^3 a^{-1} (Ein Feshkha) and 19–35 × 10^6 m^3 a^{-1} (Samar) during 2004–2011 (Guttman, 2000; HSI, 2012; Laronne Ben-Itzhak and Gvirtzman, 2005; Mallast et al., 2013a).

Additionally, smaller discharge sites with concentrated or diffuse character were found at 35 specific locations along the coastline (Fig. 8C–F). These were partly known and even measured, e.g., Qedem spring area (Fig. 8c), discharged in 2005 ca. 10 × 10^6 m^3 a^{-1} (Shalev et al., 2007). However, this number represents a minimum since we exhibited at least 3 submarine springs with an estimated sea surface diameter of ca. 10 m each that probably significantly contribute to the thermally indicated extent. A second small discharge site (Fig. 8B) matches the known Kane spring area with a measured volume of 6–9 × 10^6 m^3 a^{-1} during 2004–2005 (HSI, 2012).

Along the eastern coast 22 of our detected sites were qualitatively verified. Since discharge measurements are missing, we relied on data from an airborne thermal campaign (Akawwi et al., 2008) and information of groundwater induced landslides (Closson et al., 2010). The remaining 15 sites provide concrete indications for exact spring sites that are hitherto unreported.

The complexity of physical processes that lead to thermal anomalies prevent a sufficient extrapolation of discharge volumes to identified ungauged sites that are currently subject of ongoing investigations.

Beside evaluation of relatively coarse (30 m spatial resolution) thermal satellite data, an airborne thermal campaign was conducted in January 2011. The higher resolution of 0.5 m allows differentiating single springs and to provide a precise groundwater discharge site inventory. For the NW part of the Dead Sea coast, we could refine the satellite result to a total of 72 specific discharge sites, 42 of them belong to the terrestrial spring type (Fig. 9A), 6 are of submarine origin (Fig. 9B) and 24 belong to a hitherto for the Dead Sea unreported type of seeping springs (Fig. 9C).

By analysing type respective abundances, the major groundwater contribution originates from terrestrial springs. Both, submarine and seeping springs represent a minor but considerable fraction.

3.4. Groundwater—the hydro-bio-geochemical approach

The Dead Sea basin represents a part of the tectonical active Syrian-East African Rift System and is hence crossed by a number of faults, which may act as preferential flow paths for shallow groundwaters and ascending deep seated brines as proven in several studies along the rift (e.g., Yechieli and Bein, 2002; Mallast et al., 2011; Rosenthal et al., 2011; Siebert et al., 2012). Following the remote sensing approach to locate discharge areas and to reveal their aquifers of origin, we conducted intense sampling campaigns in areas of terrestrial but also submarine discharge locations (Ionescu et al., 2012).

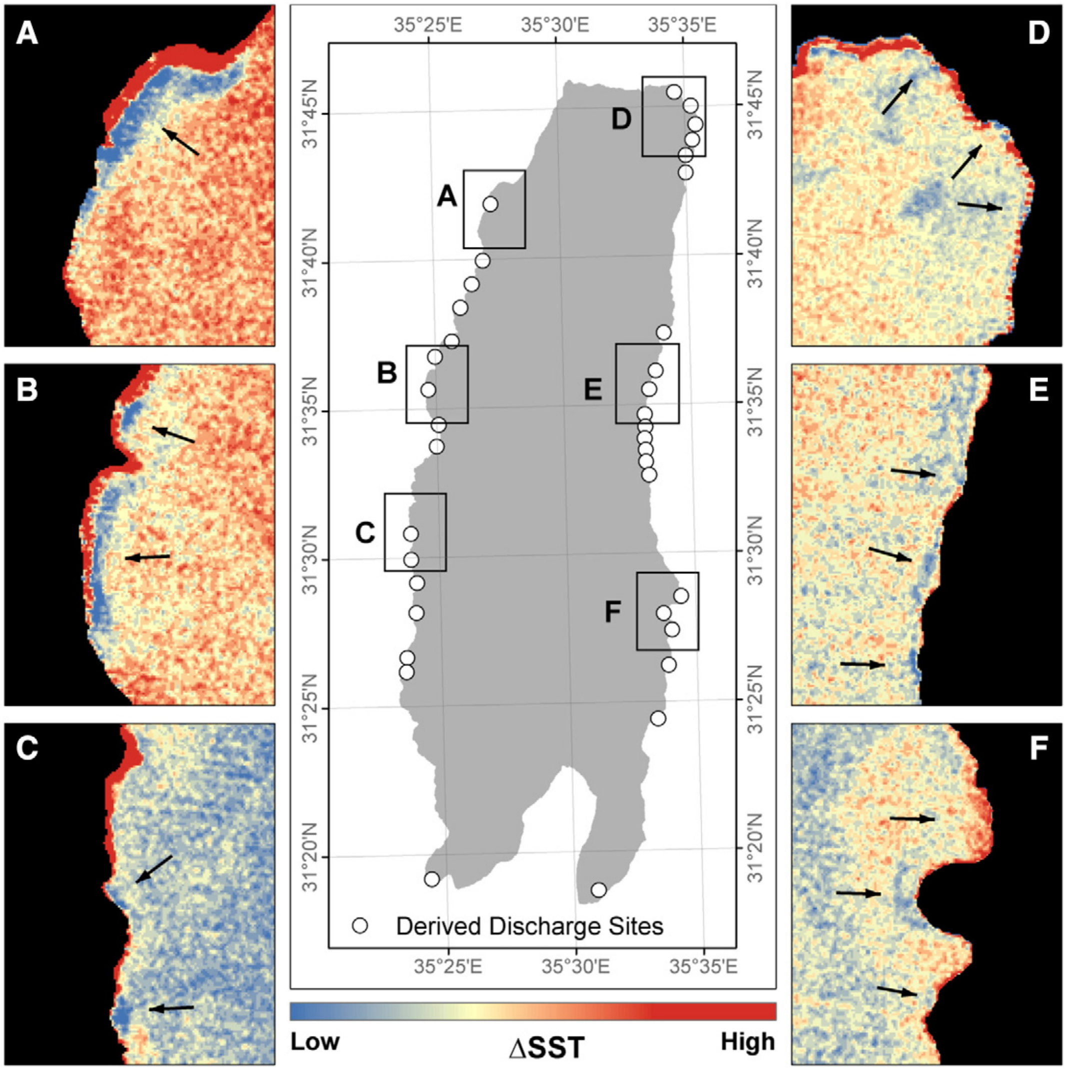

Fig. 8. Derived inflow locations (white dots) along the entire DS coast with six exemplary subsets A–F that show ΔSST values of the investigated data series of 2000–2011– colours indicate ΔSST values per pixel where blue represents small ΔSST values, which indicates stable groundwater inflow (marked with arrows) while red indicates high ΔSST values caused by external forces (e.g., seasonal air temperature course) (Mallast et al., 2013a).

It has been shown that rare earth elements including yttrium (henceforth combined to REY) in matured aquifers reveal the mineralogical composition of their infiltration rocks (e.g., Johannesson et al., 1997; Möller et al., 2003; Siebert et al., 2010). Based on reference samples from (i) prognosticated source aquifers such as the upper and lower Cretaceous aquifers, respectively, (ii) from pore waters of from DSG and (iii) the Dead Sea itself, REY-patterns in groundwaters were used to reveal the origin of spring waters (Fig. 10). However, the DSG succession consists predominantly of clay minerals and ancillary of aragonite, gypsum/anhydrite and halite (Wernicke, 2010) and, hence, shows very low bulk permeability. Consequential, groundwaters use cracks and fissures as preferential flow paths to pass the DSG. Such groundwaters about to widen virgin flow channels are strongly involved in geogenic and microbial-driven reactions with the genuine DSG minerals. These interactions intensely change the ionic and isotopic compositions and REY patterns of the passing waters (Fig. 10C), e.g., dissolution of phosphate, sulfate and carbonate minerals, microbial Fe oxidation and reduction, which occur partly simultaneously (Ionescu et al., 2012).

However, the permanent geo-bio-chemical processes, in combination with abrasion due to the passing water, enlarge pathways. In this context, very efficient is the dissolution of anhydrite/gypsum from DSG, followed by microbial sulfate reduction, with subsequent production of sulfuric acid that in turn accelerates the dissolution of abundant carbonates (Ionescu et al., 2012). The authors also found that the abundance of organic matter in the DSG sediments promote an unexpected abundance of life in the emerging groundwaters, accelerating the biochemical erosion of the DSG.

Returning to REY patterns, indeed groundwater flowing in these open (karstified) conduits, even in submarine locations about 150 m offshore, is relatively fresh (TDS <7 g l^{-1}; Ionescu et al., 2012) and exhibit clear REY-pattern of their aquifer origins. Such waters are nearly uninfluenced by admixture of pore water or mineral dissolution. By analysing the latter, it could be shown that the majority of the discharging waters originate in the upper Cretaceous aquifers (Figs. 10A, B and 1C), except the region between Mizpe Shalem and Qedem (Figs. 8C and 1A), where solely brines from lower strata (e.g., lower Cretaceous aquifer) ascend. Additionally, there are indications that the Qedem brine is admixed in variable amounts at least in the Darga/Samar spring cluster (Figs. 8B and 1A). The northern part of the Samar spring cluster shows a different water type (Guttman and Simon, 1984) with low salinity (>700 mg l^{-1} Cl^{-}) and is the water supply source to the local settlement.

The combination of these findings gives a powerful tool to generate numerical flow models that will be able to reproduce flow path networks in the DSG sediments and the characteristics of hydraulic

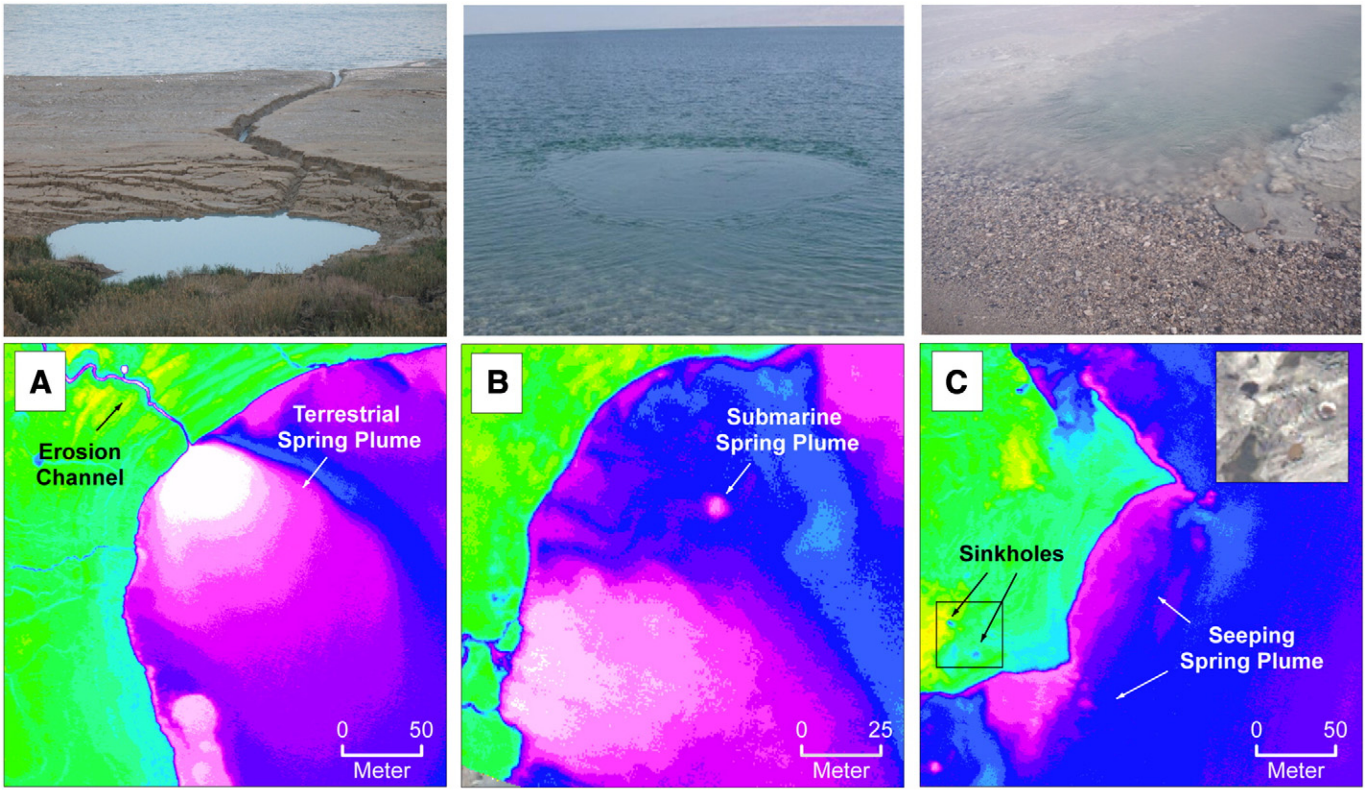

Fig. 9. Classes of thermal plumes from different types of springs—terrestrial spring (A), submarine spring (B) and from diffuse seeps (C).

connections to the lake, through the fresh–saltwater interface (Siebert et al., 2014).

3.4.1. Groundwater—the modelling approach

However, the total discharge of groundwater along the Dead Sea remains imprecise. Since we learned from thermal remote sensing investigations, groundwater discharges to a remarkable amount at ungauged sites and additionally submarine, so that discharge measurements from terrestrial springs mark the lower bound of the total groundwater inflow.

To overcome that weakness, two numerical groundwater flow models were established using Feflow to evaluate groundwater discharge at least for the upper Cretaceous aquifers on both flanks of the DS (Al-Raggad, 2009; Gräbe et al., 2013). To force the groundwater model, recharge is calculated applying a JAMS-modelling approach (chapter 3.2). The so calculated average recharge amounts to 173 × 10^6 m^3 a^{-1} (equals 45.2 mm a^{-1}) for the 3,820 km^2 large subsurface drainage basin of the upper Cretaceous aquifer in the western flank. A GIS-based modelling approach, integrating precipitation, runoff, evapotranspiration and soil retention enabled the preparation of a recharge distribution map for the subsurface basin of the upper Cretaceous aquifer in the East. It yields 109 × 10^6 m^3 a^{-1} (equals 31.7 mm a^{-1}) for the 3,427 km^2 large basin (Al-Raggad, 2009). The prevalent data scarcity required multi-component analysis of all gained data sets and information as, e.g., described by Rödiger et al. (2014) for the calibration and validation of the groundwater flow models. The results show a natural loss of groundwater to the Dead Sea from the western side of 173 × 10^6 m^3 a^{-1} and from the eastern side of 109 × 10^6 m^3 a^{-1}, values which are based on the hydraulic equilibrium between recharge and discharge. From these values, abstraction rates have to be subtracted. The exploitation of the upper Cretaceous aquifers amounts to about 50 × 10^6 m^3 a^{-1} in the west (SWITCH, 2006; PNA and PWA, 2010; PHG, 2012; Mekorot, 2012) and about 55 × 10^6 m^3 a^{-1} in the eastern flank (Al-Raggad, 2009).

Subsequent minimum total amounts flushing from upper Cretaceous aquifer (123 × 10^6 m^3 a^{-1}) in the west are in the range of the 82–96 × 10^6 m^3 a^{-1} measured by HSI for the years 2008–2011 that concern terrestrial springs at Ein Feshkha and Kane/Samar only. The remaining 27–41 × 10^6 m^3 a^{-1} may discharge via submarine springs and seeps fitting well to the 60 × 10^6 m^3 a^{-1} given by Lensky et al. (2005) for the maximum total subsurface discharge from the west. Performing the same calculation for the East reveals 54 × 10^6 m^3 a^{-1} of groundwater discharge only from the upper Cretaceous aquifer (this number does not include any contribution from the lower aquifer). Finally, the total discharge from the upper Cretaceous aquifers on both sides sums up to 177 × 10^6 m^3 a^{-1}.

By synthetically modifying the regionalized precipitation amounts, scenario analysis of recharge has been performed and shows that both sides differ considerably from each other (Fig. 11). Starting from recent amounts, a potential reduction of precipitation by maximum 30% would result in less dramatic effects on the western shoulder of the DS compared to its eastern equivalent. Following Christensen and Hewitson (2007), MMD-A1B simulations for prognostic changes of 20%–30% less annual mean precipitation in the Levant, recharge amounts are assumed to decline to 10 mm a^{-1}. However, since already today the available groundwater resources in the region do not cover the demand by far any decrease in precipitation will have tremendous socioeconomic and ecological impacts on the region.

4. Conclusion and outlook

On the basis of presented approaches, we can deduce several qualitative and quantitative key findings concerning surface- and groundwater fluxes to the Dead Sea:

- The total mean annual precipitation for the period 1979–2010 were 300 mm a^{-1} in the West and an average of 179 mm a^{-1} in the East, respectively

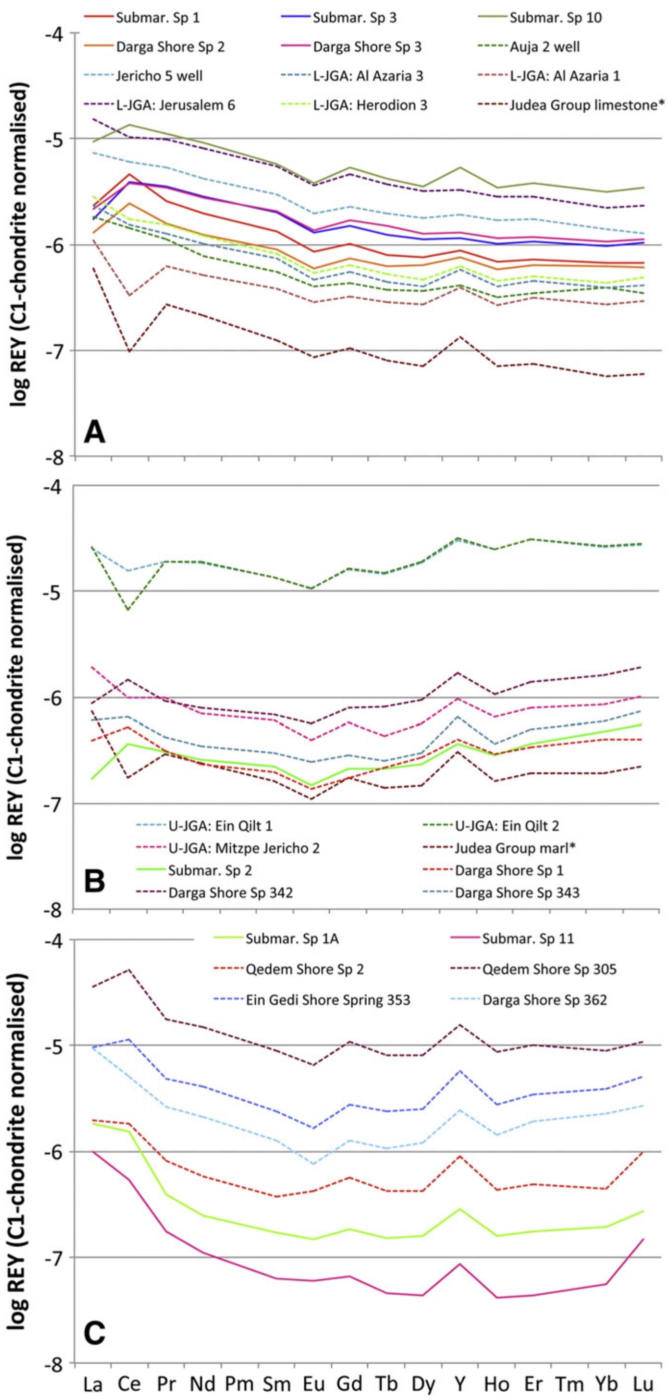

Fig. 10. Characteristic REY-pattern of reference samples and of a selection of shore- and submarine springs. Each water type shows significant features, which are unique and refer either to water from lower JGA (A), upper JGA (B) or intense contact to the DSG-sediment (C). (Ionescu et al., 2012).

- The total mean annual surface runoff from side wadis (except the Jordan River) that enter the natural DS basin amounts to approximately 40–66 × 10^6 m^3 a^{-1} (western wadis: 15 × 10^6 m^3 a^{-1}; eastern wadis: 25–51 × 10^6 m^3 a^{-1}).
- Groundwater recharge for the subsurface basins of the upper Cretaceous aquifers was calculated to be 173 × 10^6 m^3 a^{-1} in the west and 109 × 10^6 m^3 a^{-1} in the east.
- Modelled groundwater discharge volumes from upper Cretaceous aquifers amount to a total of 177 × 10^6 m^3 a^{-1} (west: 123 × 10^6 m^3 a^{-1}; east: 54 × 10^6 m^3 a^{-1}).
- Groundwater emerges at 37 concrete discharge sites around the lake either terrestrial, submarine or in a seeping form.
- Hydrogeochemical investigations in shoreline springs did reveal the origin of the groundwaters
- Geo-bio-chemical processes and water–rock interactions in the DSG sediments play the key role for highly variable hydrochemical composition of on- and offshore spring waters and the development (karstification) of conduits
- Microbial and hydrogeochemical studies proved an unexpected abundance of life in submarine springs.

Surface runoff from the east is up to three times larger than in the west. This is the result of the more than four times larger total direct surface drainage basin in the east. However, the picture turns, if surface runoffs from the direct drainage areas, groundwater recharge and groundwater discharge in and from the subsurface watersheds of the upper Cretaceous, respectively, are given in relation to the respective basin sizes. While 10.6 mm a^{-1} of runoff are generated in the 1,443 km^2 large western area, only 8.1 mm a^{-1} of runoff flow from the 6,227 km^2 large eastern basin. Likewise, recharge in the subsurface drainage basins of the upper Cretaceous aquifers is much larger in the 3,820 km^2 western large basin (45 mm a^{-1}), compared to the 3,427 km^2 large eastern one (32 mm a^{-1}). And again, groundwater discharge from the latter is not even half of the discharge from the western subsurface basin, although abstraction rates from both upper Cretaceous aquifers are comparable. The reasons may be the different mean annual precipitation amounts, which are about 300 mm a^{-1} in the western flank and only about 179 mm a^{-1} in the eastern flank of the Dead Sea.

From the executed study, we derived a number of open questions, which are suggested to be subject of future investigations.

- Does a need exist to refine the spatial resolution of precipitation data and groundwater recharge calculations to better evaluate the reasons for their dissimilar distribution and their possible relation to local synoptic systems?
- Do the hitherto unpredicted amount of discharging groundwaters from the lower Cretaceous and deeper aquifers along both flanks of the Dead Sea represent a relevant importance in the Dead Sea balance?
- What is the hydraulic connection and in how far does a biogeochemical water–rock interaction of groundwaters exists that leads to offshore spring systems, their pathways and their possible relation to neo-tectonic activities.
- As the morphogenetic evolution of offshore springs is unclear, would a high-resolution bathymetry data set provide supplementary information for numerical groundwater flow models to reduce the fuzziness of the DSG?
- In how far can we combine thermal remote sensing results with above raised questions, to find a physical based approach to evaluate submarine discharge by thermal surface anomalies?

Only by understanding all volume and mass fluxes within the Dead Sea basin an adequate basis can be developed, prerequisite for a sustainable water resources management on the basin scale.

Acknowledgement

We thank the German Ministry of Education and Research, BMBF for granting the IWRM-Project “Sustainable Management of Water Resources (Quantity and Quality) in the Dead Sea Area (SUMAR)” (grant no. 02WM0848). We are also very grateful to the Dead Sea Rescue team, Megilot Dead Sea, Omar Cohen and Jake Ben Zaken from Ein Gedi for their strong logistic support. Furthermore, we thank Dr. Gavriel Weinberger, Dr. Amir Givati and Udi Galili (Hydrological Service of Israel) for providing spring discharge data of Ein Feshkha, Kane and Samar. We are grateful to Gordana Jovan Dević, Alexandra

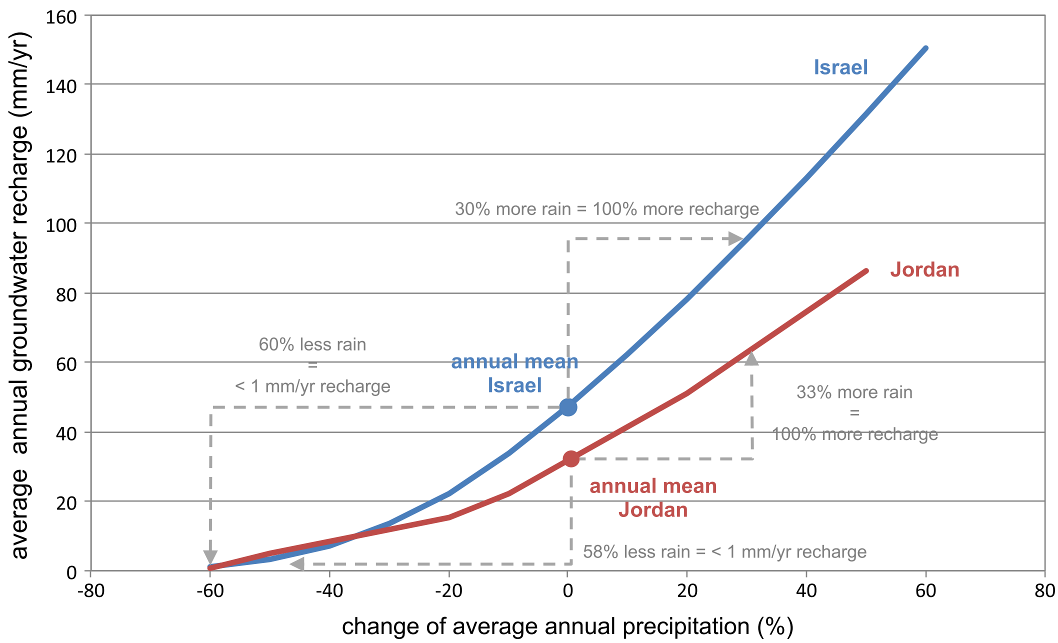

Fig. 11. Rainfall/recharge correlation for the eastern and western side of the Dead Sea, respectively.

Pavlidou and 3 further anonymous reviewers who improved the manuscript significantly.

References

Akawwi E, Al-Zoubi A, Kakish M, Koehn F, Sauter M. Using thermal infrared imagery (TIR) for illustrating the submarine groundwater discharge into the eastern shoreline of the Dead Sea-Jordan. Am J Environ Sci 2008;4:693–700.

Alkhoury W. Hydrological model of the eastern catchment of the Dead Sea. – University Göttingen, SUMAR report (unpublished, in English). 2012; 12 pp.

Al-Raggad M. GIS-based groundwater flow modeling and hydrogeochemical assessment of the northern part of the Dead Sea groundwater basin [PhD Thesis] Amman: Jordan University; 2009 [245 pp.].

Al-Taani AA. Seasonal variations in water quality of Al-Wehda Dam north of Jordan and water suitability for irrigation in summer. Arab J Geosci 2013;6:1131–40.

Al-Weshah AR. The water balance of the Dead Sea: an integrated approach. Hydrol Process 2000;14:145–54.

Asmar BN, Ergenzinger P. Dynamic simulation of the Dead Sea. Adv Water Resour 2002; 25(3):263–77.

Avrahamov N, Yechieli Y, Lazar B, Lewenberg O, Boaretto E, Sivan O. Characterization and dating of saline groundwater in the Dead Sea area. Radiocarbon 2010;52(2–3): 1123–40.

Burg A. Examination of using Ein Fesh'ha (Tzukim) spring water. Investigation of the hydrogeology system of the springs. GSI report no. 14-2005, 2005; 2006. [10 pp.].

Christensen JH, Hewitson B. (coordinating lead authors): Climate Change 2007: The Physical Science Basis. Contribution of Working Group I to the 4th Assessment Report of the Intergovernmental Panel on Climate Change. Solomon S, Quin D, Manning M, et al. (eds.). Cambridge University Press, Cambridge. 2007; 104 pp.

Closson D, Abou Karaki N, Hallot F. Landslides along the Jordanian Dead Sea coast triggered by the lake level lowering. Environ Earth Sci 2010;59(7):1417–30.

Cohen H, Laronne JB. High rates of sediment transport by flashfloods in the Southern Judean Desert, Israel. Hydrol Process 2005;19:1687–702.

Enzel Y, Agnon A, Stein M. New frontiers in Dead Sea paleoenvironmental research. Geol Soc Am Spec Pap 2006;401. [253 pp.].

Ereifeg J. Gas geochemistry and isotopic signatures in the deep thermal waters in Jordan. Freiberg Online Geol 2006;16. [256 pp.].

EXACT. Overview of Middle East Water Resources. Water Resources of Palestinian, Jordanian, and Israeli Interest. http://exact-me.org, 1998.

Frumkin A, Ezersky M, Al-Zoubi A, Akkawi E, Abueladas A-R. The Dead Sea sinkhole hazard: geophysical assessment of salt dissolution and collapse. Geomorphology 2011;134:102–17.

Gavrieli I, Yechieli Y, Halicz L, Spiro B, Bein A, Efron D. The sulfur system in anoxic subsurface brines and its implication in brine evolutionary pathways: the Ca-chloride brines in the Dead Sea area. EPSL 2001;186:199–213.

Gavrieli I, Lensky NG, Dvorkin Y, Lyakhovsky V, Gertmann I. A multi-component chemistry based model of the Dead Sea (in English). GSI-Report GSI/24/2006; 2006. [61 pp.].

Gertman I, Hecht A. The Dead Sea hydrography from 1992 to 2000. J Mar Syst 2002;35: 169–81.

Gräbe A, Rödiger T, Rink K, Fischer T, Sun F, Wang W, et al. Numerical analysis of the groundwater regime in the western Dead Sea Escarpment, Israel and West Bank. Environ Earth Sci 2013;69(2):571–85.

Greenbaum N, Ben-Zvi A, Haviv I, Enzel Y. The hydrology and paleohydrology of the Dead Sea tributaries. In: Enzel Y, Agnon A, Stein M, editors. New Frontiers in the Dead Sea Paleoenvironmental Research. Boulder, CO, USA: The Geological Society of America; 2006. [254 pp.].

Greenman A. Estimation of surface water volume and quality discharging into the Dead Sea. MSc-Thesis, Ben Gurion University of the Negev (unpublished). 2010; 105 pp.

GTZ, NRA. National water master plan of Jordan. Agrar- und Hydrotechnik GmbH ESSE. Hannover: Bundesanstalt für Geowissenschaften und Rohstoffe; 1977.

Guttman J. Hydrogeology of the eastern aquifer in the Judea Hills and Jordan Valley. In: Guttman J, editor. Multi-Lateral Project—Project 02WT9719 within the Framework of the German–Israeli–Jordanian–Palestinian Joint Research Program for the Sustainable Utilization of Aquifer Systems. Mekorot; 2000. [83 pp.].

Guttman J, Simon E. Hydrological study of the western Dead Sea shore, stage 1. Tahal Consulting Engeneers Ltd.; 1984 [67 pp. (in Hebrew)].

Gvirtzman H, Stanislyvsky E. Large-scale flow of geofluids at the Dead Sea Rift. J Geochem Explor 2000;69–70:207–11.

Holtzman R, Shavit U, Segal-Rozenhaimer M, Gavrieli I, Marei A, Farber E, Vengosh A. Quantifying Ground Water Inputs along the Lower Jordan River. J Environ Qual 2005;34(3):897–906.

HSI. Spring discharge measurements along the Dead Sea. Hydrological Service of Israel (unpublished data), Jerusalem, 2012.

Ionescu D, Siebert C, Polerecky L, Munwes YY, Lott C, Häusler S. Microbial and chemical characterization of underwater fresh water springs in the Dead Sea. PLoS One 2012;7(6): 1–29.

Johannesson KH, Stetzenbach KJ, Hodge VF. Rare earth elements as geochemical tracers of regional groundwater mixing. Geochim Cosmochim Acta 1997;61(17):3605–18.

Katz A, Starinsky A. Geochemical history of the Dead Sea. Aquat Geochem 2008;15(1–2): 159–94.

Kralisch S, Krause P. JAMS—a framework for natural resource model development and application. In: Gourbesville P, Cunge J, Guinot V, Liong S-I, editors. Proceedings of the 7th International Conference on Hydroinformatics; 2006. p. 2356–63.

Lange J. A non-calibrated rainfall–runoff model for large arid catchments, Nahal Zin, Israel. Freiburger Schriften zur Hydrologie. Freiburg i.Br. Germany: Albrecht Ludwigs Univ.; 1999. [123 pp.].

Laronne Ben-Itzhak L, Gvirtzman H. Groundwater flow along and across structural folding: an example from the Judean Desert, Israel. J Hydrol 2005;312(1–4):51–69.

Lensky NG, Dvorkin Y, Lyakhovsky V, Gertman I, Gavrieli I. Water, salt, and energy balances of the Dead Sea. Water Resour Res 2005;41:W12418. http://dx.doi.org/10.1029/2005wr004084.

Mallast U, Gloaguen R, Geyer S, Rödiger T, Siebert C. Derivation of groundwater flow-paths based on semi-automatic extraction of lineaments from remote sensing data. HESS 2011;15:2665–78.

Mallast U, Siebert C, Wagner B, Sauter M, Gloaguen R, Geyer S, et al. Localisation and temporal variability of groundwater discharge into the Dead Sea using thermal satellite data. Environ Earth Sci 2013a;69(2):587–603.

Mallast U, Schwonke F, Gloaguen R, Geyer S, Sauter M, Siebert C. Airborne thermal data identifies groundwater discharge at the north-western coast of the Dead Sea. Remote Sens 2013b;5:6361–81.

Mazor E, Levitte D, Truesdell AH, Healy J, Nissenbaum A. Mixing models and ionic geothermometers applied to warm (up to 60 °C) springs: Jordan Rift Valley, Israel. J Hydrol 1980;45:1–19.

Mekorot. Abstraction rates from Judea group aquifer. Tel Aviv, Israel: Internal database Mekorot Co. Ltd.; 2012.

Menzel L. Modellierung der Evapotranspiration im System Boden-Pflanze-Atmosphäre. Zürcher Geographische Schriften, 67. Zürich Swiss: Geographisches Institut ETH; 1997. [128 pp.].

Möller P, Rosenthal E, Geyer S, Guttman J. Rare earths and yttrium hydrostratigraphy along the Lake Tiberias–Dead Sea–Arava transform fault, Israel and adjoining territories. Appl Geochem 2003;18(10):1613–28.

Möller P, Rosenthal E, Geyer S, Guttman Y, Dulski P, Rybakov M, et al. Hydrochemical processes in the lower Jordan valley and in the Dead Sea area. Chem Geol 2007; 239(1–2):27–49.

Morin E, Jacoby Y, Navon S, Bet-Halachmi E. Towards flash-flood prediction in the dry Dead Sea region utilizing radar rainfall information. Adv Water Resour 2009;32(7): 1066–76.

Munwes Y, Laronne JB, Geyer S, Siebert C, Sauter M, Licha T. Direct measurement of submarine groundwater spring discharge upwelling into the Dead Sea. proceedings IWRM Karlsruhe; 2010.

Niemi TM, Ben-Avraham Z, Gat JR. The Dead Sea. The lake and its setting. Oxf Monogr Geol Geophys 2009;36:1–306.

Odeh T, Salameh E, Schirmer M, Strauch G. Structural control of groundwater flow regimes and groundwater chemistry along the lower reaches of the Zerka River, West Jordan, using remote sensing, GIS, and field methods. Environ Geol 2009; 58(8):1797–810.

Odeh T, Geyer S, Rödiger T, Siebert C, Schirmer M. Groundwater chemistry of strike slip faulted aquifers: the case study of Wadi Zerka Ma'in aquifers, north east of the Dead Sea. Environ Earth Sci 2010:1–14.

Oz I, Shalev E, Gvirtzman H, Yechieli Y, Gavrieli I. Groundwater flow patterns adjacent to a long-term stratified (meromictic) lake. Water Resour Res 2011;47:W08528.

PHG. Palestine Hydrology Group, Internal database; 2012.

PNA, PWA. Water supply report 2010. Palestine Water Authority; 2010 [100 pp.; www.pwa.ps].

Rödiger T, Geyer S, Mallast U, Merz R, Krause P, Fischer C, et al. Multi-response calibration of a conceptual hydrological model in the semiarid catchment of Wadi Al Arab, Jordan. J Hydrol 2014;509:193–206.

Rosenthal E, Meiler M, Flexer A. Structure-controlled groundwater flow and salinization paths in the Bet She'an and Harod Valleys, Israel. Environ Earth Sci 2011. http://dx.doi.org/10.1007/s12665-011-1313-4.

Sachse et al. The hydrology of the western Dead Sea surface drainage basin. unpublished UFZ-report, 2013; 56 pp.

Salameh E. Water Quality Degradation in Jordan (Impacts on Environment, Economy and Future Generations Resources Base). Amman: Friedrich Ebert Stiftung, Royal Society for the Conservation of Nature; 1996.

Salameh E, Al Farajat M. The role of volcanic eruptions in blocking the drainage leading to the Dead Sea formation. Environ Geol 2006;52(3):519–27.

Salameh E, El-Nasser H. Does the actual drop in Dead Sea level reflect the development of water sources within its drainage basin? Acta Hydrochim Hydrobiol 1999;27(1): 5–11.

Salameh E, El-Nasser. Changes in the Dead Sea Level and their Impacts on the Surrounding Groundwater Bodies. Acta Hydrochim Hydrobiol 2000;28:24–33.

Salameh E, Hammouri R. Sources of groundwater salinity along the flow path, Disi–Dead Sea/Jordan. Environ Geol 2008;55(5):1039–53.

Shalev E, Lyakhovsky V, Yechieli Y. Is advective heat transport significant at the Dead Sea basin? Geofluids 2007;7(3):292–300.

Shaliv E, Lyakhovsky V, Yechieli Y. Salt dissolution and sinkhole formation along the Dead Sea shore. J Geophys Res 2006;111(83):B03102.

Siebert C, Geyer S, Knöller K, Rödiger T, Weise S, Dulski P, et al. Ajloun and Golan—a transboundary groundwater resource? Transboundary aquifers: challenges and new directions. ISARM2010. Paris: UNESCO; 2010. p. 129–34.

Siebert C, Rosenthal P, Möller P, Rödiger T, Meiler M. The hydrochemical identification of groundwater flowing to the Bet She'an-Harod multiaquifer system (Lower Jordan Valley) by rare earth elements, yttrium, stable isotopes (H, O) and Tritium. Appl Geochem 2012;27:703–14.

Siebert C, Mallast U, Rödiger T, Strey M, Ionescu D, Häusler S, et al. Submarine groundwater discharge at the Dead Sea. Proceedings of SWIM23 Husum, Germany; 2014.

Stanislavsky E, Gvirtzman H. Basin-scale migration of continental-rift brines: paleohydrologic modeling of the Dead Sea basin. Geology 1999;27:791–4.

Storz-Peretz Y, Laronne JB. Morpho-textural characterization of dryland braided channels. Bull Geol Soc Am 2013;125(9/10):1599–617. http://dx.doi.org/10.1130/B30773.1.

Storz-Peretz Y, Bowman D, Laronne JB, Svoray T. Rapid incision of a small, coarse and steep fan-delta in response to base-level fall: the case of Nahal Qedem, the Dead Sea, Israel. Earth Surf Process Landf 2011;36(4):467–80.

SWITCH. 018530 - SWITCH Sustainable Water Management in the City of the Future. report of House of Water & Environment; 2006. [www.switchurbanwater.eu].

TAHAL. Red Sea - Dead Sea Water Conveyance Study Program: Best. Available Data Report, TAHAL Report IL-201280-R10-054/GSI Report GSI/19/2010; 2010. 92 pp.

Vachtman D, Laronne JB. Flow structure over bed irregularities in a straight cohesive open channel. J Hydraul Eng ASCE 2011;137(11):1335–46.

Vachtman D, Laronne JB. Hydraulic geometry of cohesive channels undergoing base level drop. Geomorphology 2013a;197:76–84.

Vachtman D, Laronne JB. Remotely sensed estimation of water discharge into the rapidly dwindling Dead Sea. Hydrological Sciences Journal 131007084053000 2013b. http://dx.doi.org/10.1080/02626667.2013.852278.

Wernicke J. Sinkholes as an indicator for groundwater flow: a remote sensing supported sedimentological study from the West Coast of the Dead Sea [Diploma-Thesis] University Leipzig; 2010 [113 pp. in English].

Yechieli Y. Fresh-saline ground water interface in the western Dead Sea area. Groundwater 2000;38(4):615–23.

Yechieli Y, Bein A. Response of groundwater systems in the Dead Sea Rift Valley to the Nuweiba earthquake: changes in head, water chemistry, and near-surface effects. J Geophys Res 2002;107(B12):2332. http://dx.doi.org/10.1029/2001JB001100.

Yechieli Y, Ronen D, Berkovitz B, Dershovitz W, Hadad A. Aquifer characteristics derived from the interaction between water levels of a terminal lake (Dead Sea) and an adjacent aquifer. Water Resour Res 1995;31(4):893–902.

Yechieli Y, Ronen D, Kaufman A. The source and age of groundwater brines in the Dead Sea area, as deduced from 36Cl and 14C. Geochim Cosmochim Ac 1996;60:1909–16.

Yechieli Y, Abelson M, Bein A, Crouvi O, Shtivelman V. Sinkhole “swarms” along the Dead Sea coast: reflection of disturbance of lake and adjacent groundwater systems. Geol Soc Am Bull 2006;118(9–10):1075–87.

Yechieli Y, Shalev E, Wollman S, Kiro Y, Kafri U. Response of the Mediterranean and Dead Sea coastal aquifers to sea level variations. Water Resour Res 2010;46:W12550. http://dx.doi.org/10.1029/2009WR008708.

Zamler D, Laronne JB. Determination of the velocity of Wadi Flood Waters Using Surface Velocity Radar. Proceedings IWRM Karlsruhe; 2010.